

Numerical Simulation of Multi-Junction Bias Circuits for Superconducting Detectors

Kenneth Segall, Juan J. Mazo, and Terry P. Orlando

Abstract—We present numerical simulations of a new biasing circuit for single photon detectors based on superconducting tunnel junctions. A single detector junction is replaced with a circuit of three junctions to achieve biasing of a detector junction at subgap currents without the use of an external magnetic field. The biasing occurs through the nonlinear interaction of the three junctions. We show nonlinear numerical simulation for different values of junction parameters and demonstrate that the biasing state is numerically stable against external fluctuations. The elimination of the external magnetic field potentially increases the capability of these types of photon detectors and eases constraints involved in the fabrication of large detector arrays.

Index Terms—Single photon detector, subgap current, superconducting tunnel junction.

I. INTRODUCTION

THE ability to do imaging while simultaneously detecting the energy and arrival time of each photon forms the ideal light detector. Applications in many fields, such as observational astronomy, materials analysis, and biophysics would benefit from such a detector. Detectors based on Superconducting Tunnel Junctions (STJ's) hold such promise, and have received attention over the past two decades [1], [2]. In these detectors, a photon with energy larger than the superconducting energy gap is absorbed in an STJ, creating quasiparticle excitations. These quasiparticles can be read out as a current pulse through the STJ. The integrated charge from this pulse can be used as a measure of the photon energy. This technology has been used successfully for photons of energy from 1 eV to 10 keV. Besides the energy resolution, these detectors also offer single photon efficiency and a large absorption count rate. Multi-pixel arrays of STJ's have been fabricated and used in applications. If two junctions are used with a single absorber, they can offer spatial imaging capabilities with only a few readout channels [3], [4].

In order to operate properly, the STJ detector must be biased at a voltage between zero and $(2\Delta/e)$, where 2Δ is the energy gap of the superconductor and e is the electron charge, a range known as the subgap region. To bias stably at subgap voltages, a

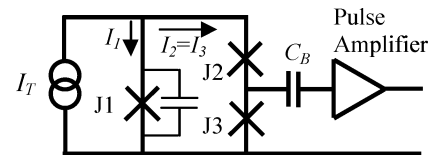


Fig. 1. Circuit schematic for magnetic-field free detector biasing; the X's represent junctions. A current I_T is applied and splits between the two branches, with the same current flowing through junctions 2 and 3. The pulse amplifier is AC coupled to junction 3. The excess quasiparticles due to photon absorption can be read out through junctions 2, 3 or both. An external capacitor can be placed in parallel with junction 1 to ease the damping requirements for the junctions.

small magnetic field is usually applied parallel to the junction in order to suppress the Josephson supercurrent. The application of a parallel field is not difficult; however it can be limiting for certain applications. For example, removing the magnetic field may open up applications involving a scanning electron microscope (SEM), such as microanalysis [5]. Presently, STJ detectors are not feasible for this application, since the applied magnetic field deflects the electron beam, necessitating large sample-detector spacing. In addition, many fields, including observational astrophysics, would benefit from very large arrays of STJ detectors. In such a case the magnetic field suppression of the supercurrent can become difficult, as small differences in junction fabrication may necessitate a slightly different field for each junction, requiring a separate electrical lead for each junction.

In this paper we show numerical simulations for a new biasing scheme for an STJ detector based on a circuit of multiple junctions which removes the need for a magnetic field. The biasing occurs through the nonlinear interaction of the detector junction(s) with other junctions in the circuit. In this paper we review the circuit concept and show the results of numerical simulations of the circuit dynamics. We simulate the circuit's stability over time and also show results for different values of the circuit parameters in order to give guidance for future designs.

II. CIRCUIT CONCEPT AND PARAMETERS

The circuit to achieve biasing without a magnetic field has been proposed previously [6] and is shown in Fig. 1. Two junctions in series (junctions 2 and 3) are placed in parallel with a third junction (junction 1). The ratio of the critical currents is 1, 0.5 and 0.5 for junctions 1, 2 and 3 respectively; other combinations are possible. A current (I_T) is applied to the three junctions as shown. To reach the desired state, the current I_T is increased until all three junctions have switched into the finite voltage state. Then the current is reduced to approximately the operating current shown in Fig. 2. Summing the voltages around the loop requires that $V_1 = V_2 + V_3$. In the desired

Manuscript received October 5, 2004. This work was supported by NSF Grant DMR-9988832, by the FEDER program through Project no. BMF2002-00113, by Colgate University and by the Colgate University Division of Natural Sciences.

K. Segall is with the Department of Physics and Astronomy, Colgate University, Hamilton, NY 13346 USA (e-mail: ksegall@mail.colgate.edu).

J. J. Mazo is with the Departamento de Física de la Materia Condensada and ICMA, CSIC-Universidad de Zaragoza, 50009 Zaragoza, Spain (e-mail: juanjo@unizar.es).

T. P. Orlando is with the Department of Electrical Engineering and Computer Science, Massachusetts Institute of Technology, Cambridge, MA 02139 USA (e-mail: orlando@mit.edu).

Digital Object Identifier 10.1109/TASC.2005.849948

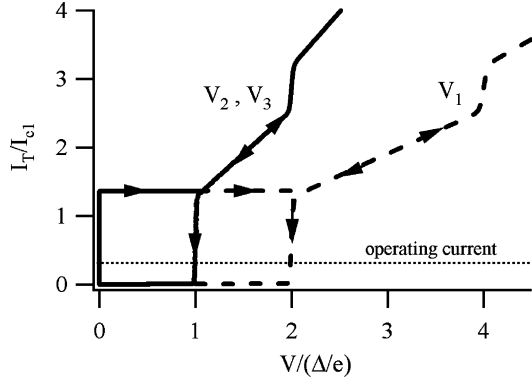


Fig. 2. Numerical simulation for the circuit shown in Fig. 1 using the full RSJ model. The total current I_T is plotted against the voltage for junctions 1 (dotted line), 2 and 3 (both solid lines). I_T is initially increased until the three junctions switch to nonzero voltage; then the current is decreased. At the operating current, junctions 2 and 3 are in the subgap region where they can function as photon detectors; here nearly all of I_T flows through junction 1.

state, junction 1 is biased at the superconducting energy gap ($V_1 = V_g = 2\Delta/e$) and junctions 2 and 3 are biased at half the energy gap ($V_2 = V_3 = V_g/2$). At this point junctions 2 and/or 3 can function as a detector; no magnetic field has been applied. The biasing occurs through the nonlinear interaction of the three junctions.

The main fabrication requirement for reaching this biasing state is that all three junctions be highly underdamped. Γ_N is the damping parameter in the normal state, equal to $\sqrt{\Phi_0/(2\pi I_C R_N^2 C)}$, where Φ_0 is the flux quantum and C is the junction capacitance. Values of $\Gamma_N < 0.05$ result in the dynamics which lead to the detector state. As discussed previously [6], this criterion is easily satisfied in niobium (Nb) junctions but is slightly more difficult for aluminum (Al) junctions. If the damping criteria cannot be met then an external, on-chip capacitor can put in parallel with junction 1; we discuss this below. The geometric inductance of the three-junction loop appears to have no major constraints; this is also discussed below.

III. NUMERICAL SIMULATION

A. Nonlinear RSJ Model

To simulate the circuit, we solve the usual RSJ model [7] for each junction with an added term for the subgap current. The normalized current through junction j is given by:

$$i_j = h_j \left(\frac{d^2 \varphi_j}{d\tau^2} + \Gamma(v_j) \frac{d\varphi_j}{d\tau} + \sin \varphi_j + i_{ss}(v_j) \right). \quad (1)$$

Here φ is the phase difference across a given junction, v is the normalized voltage across the junction ($v = d\varphi/d\tau$), $\tau = \omega_p t$ is the normalized time, ω_p is the plasma frequency, t is time, $\Gamma(v)$ is the voltage-dependent damping, h is the anisotropy parameter for the size of the different junctions, and i_{ss} is the voltage-dependent subgap current. The subscript j runs over the three junctions in the circuit. The currents i_j are normalized to the critical current of the first junction, I_{c1} . The plasma

frequency is given by $\omega_p = \sqrt{(2\pi I_c)/(\Phi_0 C)}$. The BCS subgap current is given by: [8]

$$i_{ss} = \frac{2}{I_{c1} R_n} \left(\frac{2\Delta}{eV + 2\Delta} \right)^{\frac{1}{2}} (eV + \Delta) e^{-\Delta/kT} \times \sinh \left(\frac{eV}{2kT} \right) K_0 \left(\frac{eV}{2kT} \right) \quad (2)$$

where K_0 indicates the zero-order modified Bessel function. The nonlinear damping parameter Γ is given by $\Gamma = \Gamma_N g(v)$, where $g(v)$ is the voltage-dependent damping. To account for the damping in the subgap region and for the gap rise, we use the following empirical form for $g(v)$ [9]:

$$g(v) = g_{sg} + \frac{1 - g_{sg}}{2} \left\{ 1 - \tanh \left[100 \left(1 - \frac{v_j}{v_g} \right) \right] \right\}. \quad (3)$$

Here g_{sg} is a constant damping in the subgap region and v_g is the normalized gap voltage. Equations (2) and (3) give $\Gamma(v) = g_{sg} \Gamma_N$ for $V < (2\Delta/e)$ and $\Gamma(v) = \Gamma_N$ for $V > (2\Delta/e)$.

To write the equations of the circuit we use fluxoid quantization and current conservation. Fluxoid quantization gives $(\varphi_1 - \varphi_2 - \varphi_3) = 2\pi f_{ind}$, where f_{ind} is the induced frustration in the loop formed by the three junctions. Current conservation gives $i_1 = i/2 - i_m$ and $i_2 = i_3 = i/2 + i_m$; here i_j is given by (1), $i = i_1 + i_2$, and i_m , the mesh current, is related with f_{ind} through $i_m = 2\pi \lambda f_{ind}$. The parameter $\lambda = \Phi_0/2\pi L I_{c1}$ measures the importance of induced fields; L is the geometric inductance of the loop.

B. DC Model

With the circuit biased at the desired operating point a simpler dc model can be used to predict currents and voltages at the operating point of the circuit. This DC model works well at many parameter values. In the dc model, we change (1) to the following:

$$i_j = h_j [\Gamma(v_j) v_j + i_{ss}(v_j)]. \quad (4)$$

We then use the following relations to define the DC model:

$$v_1 = v_2 + v_3 \quad (5)$$

$$i_2(v_2) = i_3(v_3) \quad (6)$$

$$i = i_1(v_1) + i_2(v_2). \quad (7)$$

Equations (5)–(7) define a system of algebraic equations which can be numerically solved. These results can be used to show how the operating point of the detector changes in response to an absorbed photon or to discuss issues of impedance and noise [6].

C. Simulation Results

The results of the model are shown in Figs. 2–5. For Figs. 2 and 3 the parameters used are $\Gamma_N = 0.02$, $h_1 = 1$, $h_2 = 0.5$, $h_3 = 0.5$, $g_{sg} = 10^{-4}$, and $\lambda = 10$. Fig. 2 shows the full dynamics of increasing and decreasing the current. To get to the operating point we increase the total current from zero to a value large enough such that all three junctions have switched. In reality the junctions will switch at different points due to fluc-

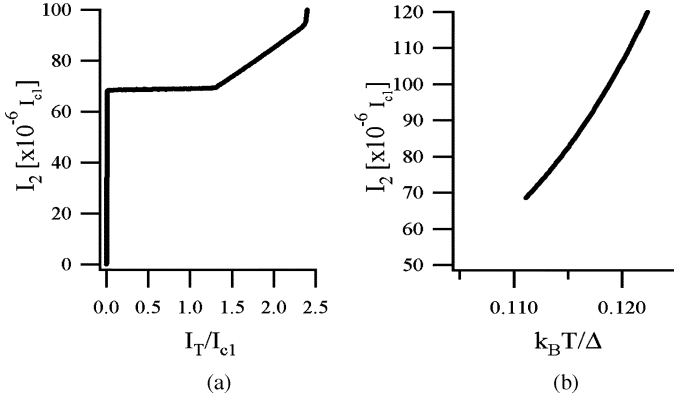


Fig. 3. Current through junctions 2 and 3 (I_2) as a function of (a) total bias current and (b) temperature. This current is only a very small fraction of I_T as seen by the scale on the y-axis. In (a), it can be seen that I_2 is independent of I_T for a range of values. The dependence on temperature shown in (b) demonstrates that I_2 can be used as a photon sensor.

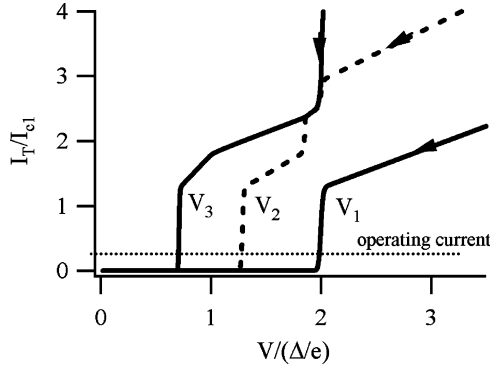


Fig. 4. Circuit simulation with critical currents of 1, 0.5 and 0.3. The voltage of junction 3 is now below the value of $(V_g/2)$. Only the decreasing current part of the simulation is shown.

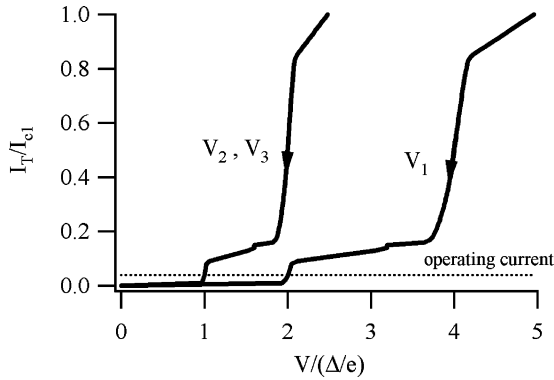


Fig. 5. Results of the model with an external capacitor in parallel with junction 1. Junction 1 has $T_N = 0.01$, while junctions 2 and 3 have $T_N = 0.15$. Again only decreasing the current is shown.

tuations, but those differences are unimportant. Once this point has been reached, the current is then decreased to the operating current shown, approximately $I_T = 0.2I_{c1}$. Following this procedure ensures the desired state will be obtained.

Fig. 2 plots the *total* current I_T on the y-axis; at the operating point shown, nearly *all* of this current I_T is flowing through junction 1. Only the small subgap current flows through junctions 2 and 3. In Fig. 3 we show this current through junctions 2 and 3, labeled I_2 for simplicity. Fig. 3(a) shows how I_2 depends on

I_T . The biasing state exists from about $I_T = 1.3I_{c1}$ down to about $0.01I_{c1}$. If I_T is decreased further, the system retraps to the zero voltage state. For noise purposes lower values of I_T are more desirable.

Fig. 3(b) demonstrates the response due to heating junctions 2 and 3, similar to an absorbed photon. The current I_2 increases with temperature as one would expect.

The circuit parameters for the case shown in Figs. 2 and 3 give a bias point exactly at $V_3 = (V_g/2)$. For Al detector junctions, a rise in the DC subgap current usually appears exactly at that voltage, making that biasing point undesirable. In such a case one can choose a different ratio of critical currents. Junctions 2 and 3 will still have the same current, because they are in series, but will lie at different voltages. Fig. 4 shows $h_1 = 1$, $h_2 = 0.5$ and $h_3 = 0.3$, allowing junction 3 to be biased at a voltage $V_3 < (V_g/2)$. The nonlinearity in both junctions 2 and 3 is included in the model. We only show it for decreasing the current; the bias current was initially increased past the switching currents.

In addition to the gap rise at $V_g/2$, Al junctions also have intrinsically higher damping than Nb junctions. As mentioned in [6], to meet the underdamped requirements in Al junctions requires fabricating a critical current density of about 5 A/cm^2 , resulting in the desired $T_N < 0.05$. This figure is independent of the junction area, which is chosen to accommodate the photon energy. If the damping criterion cannot be met, then an alternative is to place a capacitor in parallel with junction 1. This causes junction 1 to be underdamped and holds the stiff voltage bias for 2 and 3.

To simulate this we choose $T_N = 0.01$ for junction 1, but $T_N = 0.15$ for junctions 2 and 3. The value of the parallel capacitor needed to make $T_N = 0.01$ for junction 1 will depend on the junction size; the external capacitance will add in parallel with the existing junction capacitance. The results are shown in Fig. 5. The biasing state is obtained at lower bias currents, $0.02 < I_T < 0.08$, but still exists.

D. Stability of Detector State

We have found that other nonlinear states coexist in the circuit with desired detector state, which we refer to as the symmetric state since $V_2 = V_3$. These other states, which are asymmetric, are undesirable. Fluctuations can cause switching to one of the asymmetric states.

In order to check the stability of the symmetric state against external fluctuations, we added a noise term to each junction in (1). We modeled external fluctuations as being due to temperature; external magnetic field fluctuations would in principle look similar, although this has not yet been explicitly checked. We then integrated the equations for the circuit. We chose a level of noise orders of magnitude larger than expected for thermal fluctuations at typical operating temperatures. Extrapolating our results to realistic amounts of noise, we find that the symmetric state is numerically stable for times orders of magnitude longer than typical experimental times (10^4 s).

E. Importance of Induced Fields

The parameter λ measures the importance of induced fields in the 3-junction loop. The results presented thus far have $\lambda = 10$.

This corresponds to small values of the geometric inductance, of order a few pH. We have also done simulations with $\lambda = 1$ and $\lambda = 0.1$ and find negligible difference in the results. We can then also consider a simpler model, where the induced fields are completely neglected. Then the three values of the phase are constrained by:

$$\varphi_1 - \varphi_2 - \varphi_3 = 0. \quad (8)$$

The equations of the circuit are then written with only this relation and current conservation, $i_1 = i_2 + i_3$ and $i_2 = i_3$. This change results in a slightly simpler version of the full RSJ model described above in part A. This model gives identical results to the full model in all cases studied thus far. The DC model explained above can also be derived from this limit.

IV. PRACTICAL DESIGN ISSUES

To read out the excess tunneling current, a current amplifier can be AC coupled and placed in parallel with the detector junction (shown for junction 3 in Fig. 1). The blocking capacitor C_B passes signal frequencies and block DC currents. Junctions 2 and 3 are high impedance, since they biased in the subgap region, making signal collection through the low impedance current amplifier relatively efficient. The addition of the extra junctions causes excess electronic noise to the detector, which has been discussed previously [6]. In most cases the electronic noise increases by about a factor of two over the case for a single junction. This factor of two results from the fact that the overall impedance seen by the amplifier is about a factor of two smaller, since junctions 2 and 3 are effectively in parallel. Other problems may include avoiding subgap features, such as Fiske modes [10]. Here the ability to choose different ratios of critical current will help. Other subgap issues will need to be addressed with fabrication and experiments. We also note that since two of the junctions in the circuit can each be used as a detector, there are possibilities to bias a two-junction detector or even a many-pixel array in the future with this technique. This will free up electrical leads and offer more flexibility in experiment design.

V. CONCLUSIONS

We have shown simulations of a new biasing scheme for an STJ detector which removes the need for a magnetic field. Flexibility in the choice of parameters in the circuit can be used to design for a particular set of detector requirements. The elimination of the magnetic field opens up the possibility of new applications for the STJ detector as well as offering increased flexibility in scaling to larger arrays.

ACKNOWLEDGMENT

K. Segall acknowledges useful discussions with E. Trías, D. E. Prober, M. C. Gaidis, S. Friedrich, and L. Frunzio.

REFERENCES

- [1] J. Mather, "Super photon counters," *Nature*, vol. 401, pp. 654–655, 1999.
- [2] N. E. Booth and D. J. Goldie, "Superconducting particle detectors," *Supercond. Sci. Technol.*, vol. 9, pp. 493–516, 1996.
- [3] S. Friedrich, K. Segall, M. C. Gaidis, D. S. Toledano, D. E. Prober, A. E. Szymkowiak, and S. H. Moseley, "Superconducting Nb-Ta-Al-AlOx-Al X-ray detectors with spatial resolution," *Nuclear Instrum. & Methods Phys. Res.; Accelerators, Spectrometers, Detectors, Assoc. Equip.*, vol. 370, pp. 44–46, 1997.
- [4] H. Kraus, F. von-Feilitzsch, J. Jochum, R. L. Mossbauer, T. Peterreins, and F. Probst, "Quasiparticle trapping in a superconductive detector system exhibiting high energy and position resolution," *Phys. Lett. B*, vol. 231, pp. 195–202, 1989.
- [5] D. A. Wollman, S. W. Nam, G. C. Hilton, K. D. Irwin, N. F. Bergren, D. A. Rudman, J. M. Martinis, and D. E. Newbury, "Microcalorimeter energy-dispersive spectrometry using a low voltage scanning electron microscope," *J. Microscopy*, pt. 1, vol. 199, pp. 37–44, 2000.
- [6] K. Segall, J. Mazo, and T. P. Orlando. (2004) Multiple Junction Biasing of Superconducting Tunnel Junction Detectors. [Online]. Available: <http://arXiv.org/abs/cond-mat/0410072>
- [7] T. P. Orlando and K. A. Delin, *Foundations of Applied Superconductivity*. Reading, MA: Addison-Wesley, 1991.
- [8] T. Van-Duzer and C. W. Turner, *Principles of Superconductive Devices and Circuits*, Edward Arnold, London, U.K., 1981.
- [9] This constant subgap damping adds a linear current to the subgap current in (1). We chose a value for this subgap damping which adds less about 10% to the BCS subgap value. This was chosen empirically, to try to match a typical experimental I-V curve.
- [10] M. D. Fiske, "Temperature and magnetic field dependence of the Josephson tunneling current," *Rev. Modern Phys.*, vol. 36, pp. 221–224, 1964.